JOURNAL OF COMPUTATIONAL PHYSICS **40**, 361–375 (1981)

A Fully Automatic Method for Predicting Internal Reacting Flows

J. B. GREENBERG AND C. PRESSER

Department of Aeronautical Engineering, Technion–Israel Institute of Technology, Haifa, Israel

Received January 21, 1980; revised June 3, 1980

A fully automatic method for computing elliptic internal reacting flows is presented. It uses a majorant operator-splitting method for the conservation of species equations, which permits their usually problematic integration to be performed in a two-step process. For the first nonreacting stage the algorithm of Gosman *et al.* [18] is utilised, whilst the form of the second reacting stage enables the method of characteristics to be implemented so that a set of ordinary differential equations is obtained. The latter are solved using Gear's [5] method for combatting the stiffness that is frequently associated with problems involving realistic chemical kinetic schemes. Some sample results for turbulent reacting flow in a combustor with a conical burner tunnel section demonstrate the viability of the technique.

1. INTRODUCTION

The increased use of computational techniques for design and feasibility studies of combustion chambers has produced the need to develop reliable efficient algorithms to deal with the complex coupled flow and thermochemistry associated with such systems. Typically the flow will be turbulent and recirculating, with simultaneous occurrence of heat and mass transfer. With regard to the description of the chemistry involved, one of two approaches is usually opted for, particularly when hydrocarbon combustion is under consideration. Either the totality of the elementary chemical mechanism is reduced to a semiempirical *global* rate expression (see, for example, [1]), or a semiglobal approach is adopted in which the better-known elementary reaction steps are retained whilst the unknown or doubtful stages are contracted into a single global step [2, 3].

However, irrespective of the actual method used for dealing with the chemistry, the presence of chemical source terms generally leads to a numerical difficulty known as "stiffness." This problem is associated with the calculation of local species concentrations in static or dynamic systems and has been discussed extensively in the literature [4, 5]. "Stiffness" is a property that, in the current context, stems from the range of disparate time scales that are related to reactive collision times. In multicomponent, multireaction systems the *smallest* characteristic time dictates the *maximum* permissible time step for numerical integration. The latter may be prohibitively small,

0021-9991/81/040361-15$02.00/0

so that the computation of species concentrations becomes an unviable proposition. For *static* systems, where the rate equations assume the form of a set of ordinary differential equations,

$$d[n_i]/dt = R_i(n_1, n_2, ..., n_N)/M_i, \qquad i = 1, 2, ..., N, \tag{1}$$

where n_i is the molar concentration of species i, the stiff-equation algorithm of Hindmarsh and Gear [6] can capably handle the above-mentioned difficulty.

For reacting flow systems the conservation of species equations in their most general form are

$$\rho \frac{\partial m_j}{\partial t} + \rho \mathbf{v} \circ \nabla m_j = \nabla(D_j \nabla m_j) + R_j, \qquad j = 1, 2, ..., N, \tag{2}$$

where these N partial differential equations are also coupled to the conservation of mass, momentum and energy equations. For turbulent flows there is a further linkage to Eq. (2) by equations (possibly differential) that comprise a turbulence model. Particular cases of (2) have been dealt with by a number of workers, using a variety of techniques to handle "stiffness."

Dixon-Lewis *et al.* [7] proposed a method based upon certain quasi-steady-state chemical kinetic assumptions to obtain detailed species and thermal profiles in laminar, premixed flames. Their approach is, however, too problem dependent, necessitates large computer times, and is therefore unsuitable for extension to combustor studies. Smoot *et al.* [8] also considered the problem of laminar flame propagation, for methane–air flames. They treated the "stiffness" problem by linearising the chemical source terms (see also Wilde [9]). Their method suffers from the need to store and recalculate the Jacobian of the source terms at each step, as well as from excessive computer times.

Operator-splitting techniques [10] have been tested by Dwyer and Otey [11] for flame propagation problems (parabolic), and by Rizzi and Bailey [12] for inviscid, reacting flows (hyperbolic). The same sort of approach was adopted by Thomas and Wilson [13] for calculating the flow in a chemically reacting turbulent jet and by Kee and Miller [14] for determining the properties of an axisymmetric laminar jet diffusion flame. The overall performance of these methods is very satisfactory, although some large computer times are again reported (for example, [14]).

For steady-state internal reacting flows, Eqs. (2) assume an elliptic form. Kennedy and Scaccia [15] solved for laminar reacting flow in a combustor. They dealt successfully with stiffness by the following procedure. The chemical rate terms, involved in those reactions causing stiffness, are artificially suppressed by raising the mass fractions they contain to a power, α, greater than one. The governing nonlinear finite-difference equations are solved iteratively and the chemical source terms are slowly released by allowing α to tend to one as the number of iterations grows. The path which α must follow to attain unity (that is, full chemical reaction representation) is completely unknown a priori, so that the approach to this limit must be

reached in a rather tedious and time-consuming trial and error fashion. Arbib *et al.* [16] also utilised this technique for investigating high intensity confined hydrocarbon flames.

Spiegler *et al.* [17] devised a novel method for tackling "stiffness" of elliptic equations. They *estimate* the species concentration field variation during each iteration with the help of *approximate* analytic functions. However, these may be grossly in error for certain times, as evidenced by Fig. 5 of Ref. [17], where a 25% overestimate is illustrated! Although the technique is attractive in its being automatic, much computational effort must be spent at each point in the field in order to calculate local equilibrium concentrations, etc. This can be time-consuming, particularly if many species are assumed to play a role in the chemical model.

In the present work an alternative automatic method for dealing with reacting turbulent flows of an elliptic nature is discussed. It combines the positive features of some of the methods reviewed above. Some sample computed results are given for turbulent combustion in an industrial furnace with a conical burner tunnel.

2. Equations to Be Solved

The solution of the equations describing an axisymmetric turbulent reacting flow field in a steady state is considered. For such a system, Eqs. (2) and the other governing equations may be cast into the familiar form [18]

$$a_\phi \left\{\frac{\partial}{\partial z}\left(\phi \frac{\partial \psi}{\partial r}\right) - \frac{\partial}{\partial r}\left(\frac{\partial \psi}{\partial z}\right)\right\} - \frac{\partial}{\partial z}\left\{b_\phi r \frac{\partial (c_\phi \phi)}{\partial z}\right\}$$

$$- \frac{\partial}{\partial r}\left\{b_\phi r \frac{\partial (c_\phi \phi)}{\partial r}\right\} + r d_\phi = 0, \tag{3}$$

where r and z are the radial and axial coordinates; ψ is the stream function; and the functions a_ϕ, b_ϕ, c_ϕ, and d_ϕ for each dependent variable ϕ are given in Table I.

Note that the turbulence model is of the two equation variety with conservation equations for k (kinetic energy of turbulence) and $k \cdot l$, where l is the turbulence length scale. The effective dynamic viscosity is computed using [19]

$$\mu_{\text{eff}} = 0.22 \rho k^{1/2} l. \tag{4}$$

The procedure for solving Eqs. (3) involves discretising the system and consequently attention is focused on a finite number of grid points covering the whole field. The finite-difference equations are then recast as successive substitution formulae of the kind,

$$\phi_P = L_{EWNS}(\phi) + S(\phi), \tag{5}$$

TABLE I

Equation Parameters

ϕ	a_ϕ	b_ϕ	c_ϕ	d_ϕ
$\frac{\omega}{r}$	r^2	r^2	μ_{eff}	$\frac{\partial}{\partial z}(\rho w^2) - r\left[\frac{\partial}{\partial z}\left(\frac{u^2+v^2}{2}\right)\cdot\frac{\partial \rho}{\partial r} - \frac{\partial}{\partial r}\left(\frac{u^2+v^2}{2}\right)\frac{\partial \rho}{\partial z}\right] - r^2 S_w$
ψ	0	$\frac{1}{\rho r^2}$	1	$-\frac{\omega}{r}$
k	1	$\Gamma_{k,\text{eff}}$	1	$-\mu_t\left\{2\left[\left(\frac{\partial u}{\partial z}\right)^2+\left(\frac{\partial v}{\partial r}\right)^2\right]+\left[\frac{\partial u}{\partial r}+\frac{\partial v}{\partial z}\right]^2 + \left[r\frac{\partial (w/r)}{\partial z}\right]^2+\left[r\frac{\partial (w/r)}{\partial r}\right]^2\right\} + \frac{\rho k^{3/2}}{l}C_D$
lk	1	$\Gamma_{kl,\text{eff}}$	1	$-C_B l\mu_t\left\{2\left[\left(\frac{\partial u}{\partial z}\right)^2+\left(\frac{\partial v}{\partial r}\right)^2\right]+\left[\frac{\partial u}{\partial r}+\frac{\partial v}{\partial z}\right]^2 + \left[r\frac{\partial (w/r)}{\partial z}\right]^2+\left[r\frac{\partial (w/r)}{\partial r}\right]^2\right\} + kl\left\{\frac{C_s k^{1/2}\rho}{l}+\frac{\rho D_2 C_2 l[(\partial k/\partial z)^2+(\partial k/\partial r)^2]}{k^{3/2}}\right\}$
wr	1	$\mu_{\text{eff}} r^2$	$\frac{1}{r^2}$	0
m_j	1	$\Gamma_{j,\text{eff}}$	1	$-R_j$
$\bar{h}_t$	1	$\Gamma_{h,\text{eff}}$	1	$-\frac{1}{r}\frac{\partial}{\partial z}\left[\mu_{\text{eff}} r\left\{\left(1-\frac{1}{\sigma_h}\right)\frac{\partial(\bar{V}^2/2)}{\partial z}+\left(\frac{1}{\sigma_k}-\frac{1}{\sigma_h}\right)\times\frac{\partial k}{\partial z}+\sum_j\left(\frac{1}{\sigma_j}-\frac{1}{\sigma_h}\right)h_j\frac{\partial m_j}{\partial z}\right\}\right] - \frac{1}{r}\frac{\partial}{\partial r}\left[\mu_{\text{eff}} r\left\{\left(1-\frac{1}{\sigma_h}\right)\times\frac{\partial(\bar{V}^2/2)}{\partial r}+\left(\frac{1}{\sigma_k}-\frac{1}{\sigma_h}\right)\frac{\partial k}{\partial r}+\sum_j\left(\frac{1}{\sigma_j}-\frac{1}{\sigma_h}\right)h_j\frac{\partial m_j}{\partial r}\right\}\right]$

Note. $C_D = 0.416$, $C_B = 1.0$, $C_s = 0.057$, $D_2 = 1.0$, $C_2 = 1.0$.

where the convection–diffusion operator L_{EWNS}, of the form

$$L_{EWNS}(\phi) = A_E\phi_E + A_W\phi_W + A_N\phi_N + A_S\phi_S, \tag{6}$$

and the source term operator S (derived from the terms d_ϕ in (3)) relate the values of the variables at a node P to those at adjacent nodes, E, W, N, S (see Fig. 1). Full details are reported in the text of Gosman *et al.* [18]. The formulae are utilised

iteratively using the Gauss–Seidel method, with appropriate under-relaxation to aid stability by ensuring that exaggerated variations in ϕ_P do not occur from one iteration to the next.

With regard to the chemical source terms, it is supposed that $\bar{P}$ is the number of elementary and/or global reactions postulated to be occurring,

$$\sum_{j=1}^{N} \nu_{ij} A_j \rightleftharpoons \sum_{j=1}^{N} \nu'_{ij} A_j \qquad (i = 1, 2, \ldots, \bar{P}), \tag{7}$$

where ν_{ij} and ν'_{ij} are the stoichiometric coefficients of species A_j occurring as a reactant or a product, respectively, in reaction i.

Thus, in general, the species production (or depletion) terms are of the functional form

$$M_j(dn_j/dt)_{\text{chem.}} = R_j \equiv R_j(m_1, \ldots, m_N, T, \nu_{1j}, \nu_{2j}, \ldots, \nu_{\bar{P}j}, \nu'_{1j}, \ldots, \nu'_{\bar{P}j}) \quad (j = 1, 2, \ldots, N). \tag{8}$$

It is precisely these terms that give rise to the problem of "stiffness," which, in the iterative solution using (5), exhibits itself in the form of excessively high temperatures, and mass fractions that are greater than one or negative. The subsequent disruptive influence upon the other coupled flow variables is inevitable.

3. Procedure for Handling Stiffness

The numerical method suggested here for dealing effectively with stiffness is conceptually a split-operator technique (a full theoretical treatment of such methods can be found in the text of Yanenko [10]). Essentially, the finite-difference operator, replacing the differentials, is split in a way that implies that only certain terms of the original differential equation are represented for a fraction of a step, whilst the remaining terms make their contribution in order to complete the step. This approach is sometimes referred to as the majorant method. It is (numerically) consistent only after a whole step is made, but not at the intermediate stage.

In the current context, the conservation of species equations are split into a "fluid mechanical" part and a "chemical reaction" part in the following way (here, for the sake of clarity, the *differential equations* have been split, although formally it is their finite-difference counterparts that receive this treatment):

$$\frac{\partial}{\partial z}\left(m_j \frac{\partial \psi}{\partial r}\right) - \frac{\partial}{\partial r}\left(m_j \frac{\partial \psi}{\partial z}\right) - \frac{\partial}{\partial z}\left\{\Gamma_{j,\text{eff}} r \frac{\partial}{\partial z} m_j\right\} - \frac{\partial}{\partial r}\left\{\Gamma_{j,\text{eff}} r \frac{\partial m_j}{\partial r}\right\} = 0, \tag{9}$$

$$\frac{\partial}{\partial z}\left(m_j \frac{\partial \psi}{\partial r}\right) - \frac{\partial}{\partial r}\left(m_j \frac{\partial \psi}{\partial z}\right) - rR_j = 0. \tag{10}$$

Furthermore, rearrangement of (10), accompanied by use of the definition of the stream function and the continuity equation, enables it to be rewritten as

$$u\frac{\partial m_j}{\partial z}+v\frac{\partial m_j}{\partial r}=R_j/\rho. \tag{11}$$

Using characteristics theory this partial differential equation may be transformed into a simple ordinary differential equation

$$\frac{dm_j}{dt}=R_j/\rho, \tag{12}$$

where

$$\frac{d}{dt}=u\frac{\partial}{\partial z}+v\frac{\partial}{\partial r}. \tag{13}$$

Now the finite-difference solution of (9) represents the first fraction of a step, whilst the solution of (12) completes the step. In physical terms one may interpret this two-stage process as follows. Consider an elementary finite-difference cell, such as that in Fig. 1. In the first stage of the splitting fluid is permitted to convect and diffuse into and out of the cell. At the second stage the cell behaves like a static reactor whose current chemical contents react with one another according to (7). (Note that the method proposed by Spiegler *et al.* [17] attacks the stiffness problem solely from this physical viewpoint. Actually, their technique can be envisaged as a sort of majorant method in disguise.)

The advantage of recasting the second stage into an ordinary differential equation, Eq. (12), is apparent. The wide range of typical time scales (associated with the source term) which cause stiffness now appear *only* in this equation. Solution of stiff ordinary differential equations can be carried out numerically with ease, using the (now standard) technique of Gear [5].

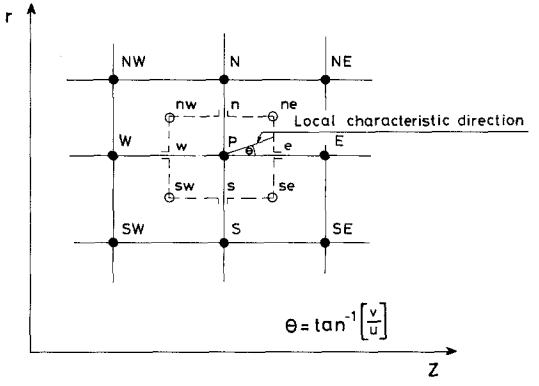

FIG. 1. Elementary finite-difference cell.

Both the physical and formal descriptions of splitting dictate the following two-step calculation procedure for the mass fractions of all reactive species:

(i) Determine the mass fraction of species j that will accumulate in a cell, surrounding point P, through convection and diffusion only; i.e.,

$$m^*_{j,p} = L_{EWNS}(m_j). \tag{14a}$$

(ii) Using $m^*_{j,p}$ calculate the mass fraction produced in the "reactor" surrounding P, by chemical reaction proceeding for a typical residence time,

$$m_{j,p} = m^*_{j,p} + \int_0^\tau R_j/\rho \, dt. \tag{14b}$$

Step (i) is carried out in the regular successive substitution manner. For step (ii) the set of N ordinary differential equations (12) must be solved simultaneously. If the problem of stiffness exists, these are integrated numerically with respect to time using the algorithm of Hindmarsh [6] for stiff ODEs. The typical residence time, τ, is based upon the cell's dimensions and the fluid velocity at the point P in the following way.

It is, first of all, noted that stage (ii) represents integration along a characteristic line defined by

$$dr/dz = v/u \tag{15}$$

The length of this line from the point P to its intersection with the boundary of the cell surrounding P is given by

$$\beta = \tau \sqrt{u^2 + v^2}. \tag{16}$$

(assuming that the velocity is locally constant). Now, referring to Fig. 1 and considering the quadrant (P, n, ne, e) only, it can be deduced that

$$\begin{aligned} \beta &= \left|\frac{\Delta z}{u}\right| \sqrt{u^2 + v^2} \qquad \text{if } \tan^{-1}\left|\frac{v}{u}\right| \leqslant \tan^{-1}\left|\frac{\Delta r}{\Delta z}\right| \\ &= \left|\frac{\Delta r}{v}\right| \sqrt{u^2 + v^2} \qquad \text{if } \tan^{-1}\left|\frac{v}{u}\right| \geqslant \tan^{-1}\left|\frac{\Delta r}{\Delta z}\right|, \end{aligned} \tag{17}$$

where Δr and Δz are the lengths of Pn and Pe, respectively. Hence, combining (16) and (17), the upper limit of the integral in (14b) is found to be

$$\tau = \min\left\{\left|\frac{\Delta z}{u}\right|, \left|\frac{\Delta r}{v}\right|\right\}. \tag{18}$$

The mass fractions obtained in the above manner are precise (to within the accuracy of the algorithm) in relation to conditions currently prevailing at a given iteration in

the elementary cell. Thus, irrespective of the particular initial chemical contents of the cell at the beginning of an iteration, the solution of (12) will always yield physically meaningful values for the mass fractions since no timewise solution can permit otherwise. This is due to the correct integration that is carried out for the time period corresponding to one iteration. There is no need to waste computational effort on local chemical equilibrium calculations (see [17]) since if this state is to be attained within a "reactor" the integration automatically drives the concentrations to their equilibrium values. In addition, the versatility of the solution procedure for the *complete* set of dependent variables is enhanced, since examination of different combustible mixtures simply entails supplying appropriate thermochemical data for all species present, together with a single new subroutine containing the chemical kinetics described by (7).

An apparent disadvantage of the above-described approach is the large number of ordinary differential equations that must be integrated. If the physical domain is covered with a mesh of $NX \times NY$ internal points, then the total number of equations is $N * NX * NY$ per iteration. In order to reduce this work load, the species concentration equations can be solved at preselected mesh points only. Values of mass fractions at the remaining points can then be supplied by interpolation. (In the results to be presented Lagrangian interpolation was used, although this may be impoved.) It was found that this line of attack significantly reduced the computer time without jeopardizing the convergence to a final solution (see also Section 4).

The major advantage of the approach is that, in contrast to other methods, it renders the entire solution procedure for internal reacting flows automatic, without any necessity for programmer–computer interaction at intermediate stages of the calculation. Experience has also shown that the converged solution is attained in a relatively small number of iterations.

4. Boundary Conditions and Initial Guesses

The ellipticity of the governing differential equations dictates the need to specify boundary conditions at all points surrounding the flowfield.

With particular reference to the combustion chamber for which results will be presented (see Fig. 2): at the inlet the axial velocity was specified according to the one-seventh law for fully developed turbulent pipe flow. The radial velocity was zero, whilst the tangential velocity was either zero or assumed uniform in such a way as to produce a specified swirl number,

$$SN = J_\phi / J_x \bar{R}; \qquad J_\phi = \int_0^{\bar{R}} \rho r^2 uw dr; \qquad J_x = \int_0^{\bar{R}} \rho r u^2 dr. \tag{19}$$

The inlet stream function and vorticity were computed from the axial velocity profile.

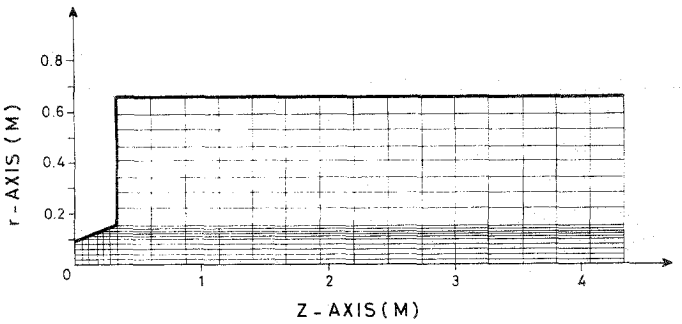

FIG. 2. The combustion chamber and finite-difference mesh.

The distributions of k and l were taken to be those pertaining to turbulent flow in pipes:

$$l/R = 0.14 - 0.08(r/\bar{R})^2 - 0.06(r/\bar{R})^4, \tag{20}$$

$$k = (0.049\, U_{\max})^2[1 + 4(r/\bar{R})^2]. \tag{21}$$

Temperature and concentration distributions at the inlet were uniform.

Along the centerline the radial gradients of all dependent variables are zero, except for the stream function, which itself is given the value zero there.

On the combustor's walls the velocity vanishes so that ψ assumes an appropriate constant value. Due to the very steep gradients of ω/r, k and l in the vicinity of the wall a special procedure is required in order to obtain reasonable accuracy in that region without necessitating the use of many extra meshpoints. A technique was adopted in which the elliptic field is matched with an analytically described boundary layer close to the wall. Full details are given by Arbib *et al.* [16]. The combustor wall is supposed to be adiabatic and impermeable to mass fluxes, so that concentration and temperature gradients normal to the wall are zero. A second order finite difference approximation for the gradient of the mass fractions is desirable (see [16]) with the mesh being arranged so that the points *nw*, *n*, *ne* (see Fig. 1) lie on the wall.

Finally, at the exit plane the axial gradients of all the dependent variables were assumed to vanish.

To overcome the problem of the sensitivity of convergence to the initial field distributions the following procedure was found to be effective. The vorticity, k and l were assigned a constant nonzero value (taken from the inlet) throughout the entire field. Any intermediate reaction products were likewise designated an arbitrary initial value everywhere (of the order of 10^{-3}–10^{-4}). The stream function and tangential velocity were distributed linearly with respect to normalised distances. Similarly, the temperature, reactants and products were spread linearly between their unburnt and (calculated) burnt adiabatic flame values.

It seems to be advisable to initially obtain a cold, nonreacting flow solution,

assuming constant density. The chemistry is then "turned on" so that simultaneous iteration on *all* the variables is performed, until convergence is attained. Following these guidelines has proved, so far, to be failsafe. However, the question as to whether this is the optimum that can be done in terms of convergence rates remains open for such strongly nonlinear problems.

Finally, a comment on the use of interpolation to calculate the species concentrations at preselected meshpoints is in place. (It will be remembered that this procedure reduces the large number of ordinary differential equations that must be integrated at each iteration.) The worst errors are likely to be incurred in regions (usually the reaction zone) where the *actual* local behaviour of the species least complies with the interpolating polynomial. However, the converged solutions thus obtained provide an excellent initial "guess" for a further short round of iterations in which the species conservation equations are evaluated at *all* mesh points, with no interpolation. This approach is particularly recommended if the chemistry is modelled using a detailed elementary reaction mechanism involving small uncertainties in the rate constants. For global or semiglobal kinetic modelling such uncertainties are large and, as a consequence, only general *qualitative* characteristics of the reacting flow can be of interest. In such instances, the final round of integration of the ordinary differential equations at all mesh points is probably unnecessary. Numerical experience has shown that, although the "smearing" induced by (here, 4 point Lagrangian) interpolation can lead, *at the worst*, to errors of up to 40% in the mass fractions (relative to those computed using integration), the overall quantitative picture was not affected.

5. Calculated Results

The fully automatic computational procedure was used to examine the influence of geometric factors upon a variety of furnace tunnel burners. A detailed discussion of this study is given elsewhere [20]. Here some sample results are presented to illustrate the viability of the numerical technique.

The chemical kinetic scheme that was utilized is based upon the semiglobal approach and considers the burning of a premixed gasoil–air mixture as occurring according to a three-step model:

$$C_{15}H_{30} + \frac{15}{2}O_2 \rightarrow 15CO + 15H_2, \tag{22}$$

$$CO + \frac{1}{2}O_2 \rightarrow CO_2, \tag{23}$$

$$H_2 + \frac{1}{2}O_2 \rightarrow H_2O. \tag{24}$$

A similar model has been adopted by Arbib *et al.* [16] for kerosene–air combustion. The semiempirical rate expressions for these three steps are:

$$-\frac{d}{dt}[C_{15}H_{30}] = 1.2 \times 10^6 \exp\left(-\frac{9195}{RT}\right)[C_{15}H_{30}]^{0.5}[O_2], \tag{25}$$

$$-\frac{d}{dt}[CO] = 1.3 \times 10^{14} \exp\left(-\frac{30000}{RT}\right)[CO][O_2]^{0.5}[H_2O]^{0.5}, \tag{26}$$

$$\frac{d}{dt}[H_2O] = \frac{8 \cdot [H_2]}{[CO]}\frac{d[CO_2]}{dt}. \tag{27}$$

The hydrocarbon attack rate, (25), is a modified version of that given by Schefer and Sawyer [21] for the oxidation of C_3H_8. Expression (26) was culled from Howard *et al.* [22], while the work of Fenimore and Jones [23] is the source of (27).

The combustion chamber consists of a small burner tunnel section followed by a large furnace section, Fig. 2. The finite-difference mesh is constructed so as to give good resolution in the tunnel section where the flame is anticipated to stabilize. The combustor's walls are adiabatic and impervious to mass transfer. At the inlet the fuel/air mixture is in stoichiometric proportions; it enters the burner at 298 K with a velocity of 10 m/sec.

The integration domain was covered with a mesh of 20×17 internal points. Sample contours for a typical conical burner tunnel section of semiangle 11.6 degrees are shown in Figs. 3, 4 and 5, where the temperature, oxygen and carbon monoxide distributions are exhibited. The flame zone is clearly delineated by the temperature contours. The carbon monoxide profile along the centerline behaves typically, attaining a maximum when reactions (22) and (23) are equally competing, and subsequently falling off as the combustion products tend to their equilibrium values. Since the fuel/oxygen ratio is stoichiometric the oxygen is almost completely consumed by the time the furnace is reached.

In Fig. 6 the streamlines are plotted for the flow. Note the region of recirculation in the conical section. For Fig. 7 swirl has been included, the swirl number being unity. The effect of swirl is pronounced—it produces a large recirculating region along the axis that sweeps back burnt gas products to cause more rapid heating inside the tunnel. The consequent distortion of the flame is illustrated in Fig. 8, where the corresponding temperature profiles are presented (see also [24]).

The converged solutions for all the dependent variables were obtained in about 1500 iterations (a relative error of 10^{-4} was demanded), with a total time of about $1\frac{1}{2}$ hr CPU time on an IBM 370/168 computer—a time that is not unreasonable for a detailed calculated such as this.

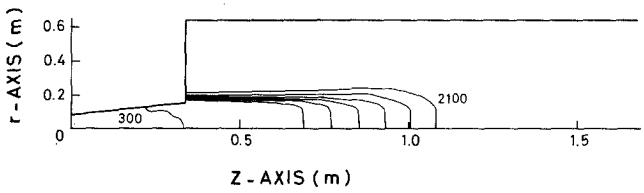

FIG. 3. Temperature distribution (K); contour increments, $\Delta T = 300$ K.

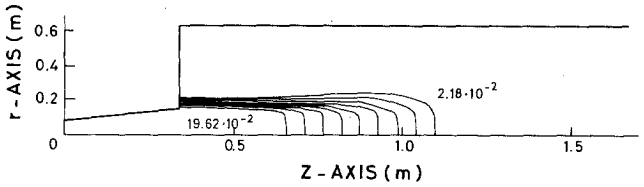

FIG. 4. Oxygen mass fraction distribution; contour increments, $\Delta m_{O_2} = 2.18 \times 10^{-2}$.

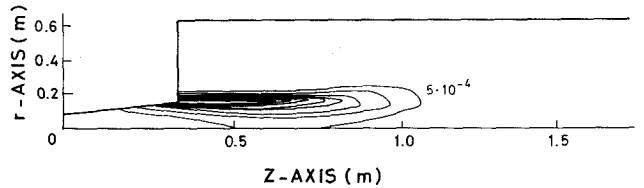

FIG. 5. Carbon monoxide mass fraction distribution; contour increments, $\Delta m_{CO} = 5 \times 10^{-4}$.

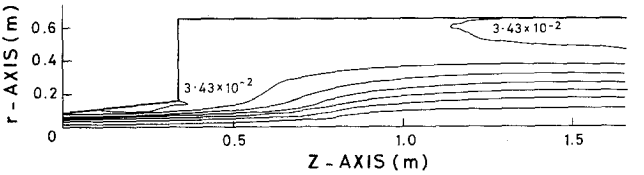

FIG. 6. Stream function contours; no swirl; contour increment, $\Delta\psi = 5 \times 10^{-3}$ kg/sec.

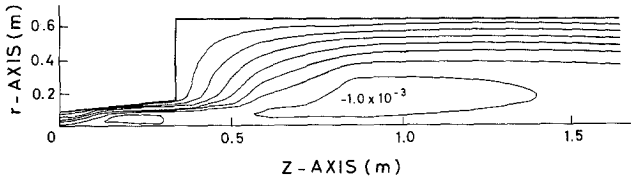

FIG. 7. Stream function contours; swirl number 1, contour increments, $\Delta\psi = 5 \times 10^{-3}$ kg/sec.

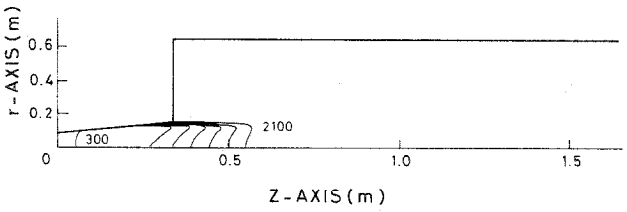

FIG. 8. Temperature distribution (K); contour increments; $\Delta T = 300$ K, swirl no. 1.

5. CONCLUSIONS

An improved method for calculating elliptic internal reacting flows has been presented. It makes use of an operator-splitting technique and Gear's [5] method for integrating stiff ordinary differential equations. It is fully automatic, versatile and efficient and, hence, may be readily incorporated into design and feasibility studies of combustion chambers.

APPENDIX: NOMENCLATURE

$a_\phi, b_\phi, c_\phi, d_\phi$	coefficients defined in Table I
A_E, A_W, A_N, A_S	coefficients in Eq. (6)
D_i	diffusion coefficient of species i
$\tilde{h}_t$	total enthalpy
J_ϕ, J_x	defined in Eq. (19)
k	turbulent kinetic energy
l	turbulence length scale
L_{EWNS}	finite-difference operator
m_i	mass fraction of species i
M_i	molecular weight of species i
n_i	moles/cm^3 of species i
N	number of species
P	pressure
$\bar{P}$	number of reactions
R	universal gas constant
$\bar{R}$	combustor inlet radius
R_j	source term of species j
r	radial coordinate
S	source term operator
SN	swirl number

t	time
T	temperature
$\mathbf{v} = (u, v, w)$	velocity
z	axial coordinate
Γ_{eff}	diffusion-type coefficients
A_j	species j
ν_{ij}, ν'_{ij}	stoichiometric constants
σ_h, σ_j	Prandtl and Schmidt numbers
ψ	stream function
ρ	density
μ_{eff}	effective viscosity
τ	residue time
ω	vorticity
$\Delta r, \Delta z$	increments of r and z, respectively
β	characteristic line length

REFERENCES

1. A. S. NOVICK, G. A. MILES, AND D. G. LILLEY, *J. Energy* **3** (1979), 95.
2. R. B. EDELMAN AND O. F. FORTUNE, AIAA Paper No. 69–86, 1969.
3. R. A. ALTENKIRCH AND A. M. MELLOR, Report No. PURDU-CL-75-01, Purdue University, West Lafayette, Indiana, 1975.
4. L. LAPIDUS AND J. H. SEINFELD, "Numerical Solution of Ordinary Differential Equations," Academic Press, London/New York, 1971.
5. W. C. GEAR, "Numerical Initial Value Problems in Ordinary Differential Equations," Prentice–Hall, Englewood Cliffs, N.J., 1971.
6. A. C. HINDMARSH, Lawrence Livermore Lab., UCRL-51186, 1972.
7. G. DIXON-LEWIS, F. A. GOLDSWORTHY, AND J. B. GREENBERG, *Proc. Roy. Soc. London Ser. A* **346** (1975), 261.
8. L. D. SMOOT, W. C. HECKER, AND G. A. WILLIAMS, *Combust. Flame* **26** (1976), 323.
9. K. A. WILDE, *Combust. Flame* **18** (1972), 43.
10. N. N. YANENKO, "The Method of Fractional Steps," Springer-Verlag, New York, 1971.
11. H. DWYER AND G. OTEY, AIAA Paper No. 78–946, 1978.
12. A. W. RIZZI AND H. E. BAILEY, *in* "Proceedings, AIAA Second Computational Fluid Dynamics Conference, Hartford, Conn., 1975," p. 38.
13. P. D. THOMAS AND K. H. WILSON, *in* "Proceedings, AIAA Second Computational Fluid Dynamics Conference, Hartford, Conn., 1975," p. 124.
14. R. J. KEE AND J. A. MILLER, *AIAA J.* **16** (1978), 169.
15. L. A. KENNEDY AND C. SCACCIA, *in* "Numerical Methods in Fluid Dynamics" (C. A. Brebbia and J. J. Connor, Eds.), p. 220, Pentech Press, London, 1974.
16. H. A. ARBIB, Y. GOLDMAN, J. B. GREENBERG, AND Y. M. TIMNAT, *Combust. Flame* **38** (1980), 259.
17. E. SPIEGLER, M. WOLFSHTEIN, AND Y. M. TIMNAT, *Acta Astronautica* **1** (1974), 935.
18. A. D. GOSMAN, W. M. PUN, A. K. RUNCHAL, D. B. SPALDING, AND M. WOLFSHTEIN, "Heat and Mass Transfer in Recirculating Flows," Academic Press, London/New York, 1969.
19. M. WOLFSHTEIN, Israel J. *Tech.* **8** (1970), 87.
20. C. PRESSER, Y. GOLDMAN, J. B. GREENBERG, AND Y. M. TIMNAT, in preparation.

21. R. W. SCHEFER AND R. F. SAWYER, NASA CR-2785, 1976.
22. J. B. HOWARD, G. C. WILLIAMS, AND D. H. FINE, *in* "Proceedings, Fourteenth Symposium (International) on Combustion," p. 975, The Combustion Institute, 1973.
23. C. P. FENIMORE AND G. W. JONES, *J. Phys. Chem.* **63** (1959), 1834.
24. C. PRESSER, "Influence of Geometric and Kinematic Factors on Flame Configuration and Combustion Performance in Industrial Furnaces," D.Sc. thesis, Department of Aeronautical Engineering, Technion–Israel Institute of Technology, Haifa, Israel, 1980.